Cross sections and oscillator strengths for electron-impact excitation of the $\tilde{A}\,^1B_1$ electronic state of water

P. A. Thorn, M. J. Brunger, P. J. O. Teubner, N. Diakomichalis, and T. Maddern
ARC Centre for Antimatter-Matter Studies, SoCPES, Flinders University, GPO Box 2100, Adelaide, South Australia 5001, Australia

M. A. Bolorizadeh
ARC Centre for Antimatter-Matter Studies, SoCPES, Flinders University, GPO Box 2100, Adelaide, South Australia 5001, Australia and Faculty of Science, Shahid Bahonar University of Kerman, Kerman, Iran 76169-133

W. R. Newell
Department of Physics and Astronomy, University College London, Gower Street, London WC1E 6BT, United Kingdom

H. Kato, M. Hoshino, and H. Tanaka
Physics Department, Sophia University, Chiyoda-ku, Tokyo 102-8554, Japan

H. Cho
Physics Department, Chungnam National University, Daejeon 305-764, Republic of Korea

Y.-K. Kim
National Institute of Standards and Technology, Gaithersburg, Maryland 20899-8422

(Received 25 October 2006; accepted 21 December 2006; published online 9 February 2007)

The authors report absolute differential and integral cross section measurements for electron-impact excitation of the $\tilde{A}\,^1B_1$ electronic state of water. This is an important channel for the production of the OH ($\tilde{X}\,^2\Pi$) radical, as well as for understanding the origin of the atmospheric Meinel [Astrophys. J. **111**, 555 (1950)] bands. The incident energy range of our measurements is 20–200 eV, while the angular range of the differential cross section data is 3.5°–90°. This is the first time such data are reported in the literature and, where possible, comparison to existing theoretical work, and new scaled Born cross sections calculated as a part of the current study, is made. The scaled Born cross sections are in good agreement with the integral cross sections deduced from the experimental differential cross sections. In addition they report (experimental) generalized oscillator strength data at the incident energies of 100 and 200 eV. These data are used to derive a value for the optical oscillator strength which is found to be in excellent agreement with that from an earlier dipole (e,e) experiment and an earlier photoabsorption experiment. © *2007 American Institute of Physics*. [DOI: 10.1063/1.2434166]

I. INTRODUCTION

Electron collisions are fundamental processes in many phenomena involving water molecules. These include understanding the observed emissions from cometary atmospheres,[1] in modeling control processes of plasma techniques that seek to ameliorate pollution from fossil fuel combustion,[2] and understanding the origin of the important atmospheric Meinel bands.[3,4] In addition, the initial physical stage of radiation interaction with biological matter can be understood on the basis of the analysis of the track structure caused by charged particles. The knowledge of electron interactions with water molecules is therefore vital in understanding radiation damage.[5]

An excellent summary of the available cross section data for electron scattering from water (H_2O) molecules is given in the recent review of Itikawa and Mason.[6] These authors noted that "to date no electron-beam measurements have reported absolute values of the (electronic state) excitation cross sections of H_2O." This fact prevented Itikawa and Mason[6] from providing a recommended set of values, which they considered to be a serious problem since "electronic excitation is important in planetary atmospheres, plasmas, and radiation chemistry." As a consequence they noted that "experiments and refined theory are urgently needed" and the results we report here are a small step in trying to overcome this deficiency. From a theoretical perspective there are, in fact, several calculations, using different methods, available in the literature for a small subset of the electronic states of H_2O. These include the *R*-matrix calculations by Morgan[7] and Gorfinkiel *et al.*[8] for the low-lying $^3B_1$, $^1B_1$, $^3A_1$, and $^1A_1$ electronic states, the complex Kohn results by Gil *et al.*[9] again for the same $^3B_1$, $^1B_1$, $^3A_1$, and $^1A_1$ states, the distorted-wave Born calculations by Lee *et al.*[10,11] for a couple of the $^3A_1$ states, and a Schwinger multichannel method result,[12] also for the lowest-lying $^3A_1$ electronic state. This apparent lack of comprehensive theoretical scattering work is not really surprising as water possesses both a strong

permanent dipole moment and a significant dipole polarizability, which makes it a real challenge for current-state-of-the-art scattering calculations. Indeed even a good description for the target states is nontrivial here.[9] In general, with some notable exceptions, most of the theory results report integral cross sections (ICSs) and there are significant quantitative differences found between the results from the different methods. This latter observation provides further impetus for the present work.

One of us developed simple scaling methods of Born cross sections to calculate reliable integral cross sections for electron-impact excitation of neutral atoms.[13] The same scaling method was also found to provide integral excitation cross sections for H_2 in good agreement with available experimental data, as is shown in the preceding article[14] (referred to as Paper I hereafter). We show in this article that the scaled Born cross sections for the excitation to the $\tilde{A}\,^1B_1$ state of H_2O are in good agreement with integral cross sections derived from the experimental differential cross sections (DCSs) presented later. In addition, we demonstrate the validity of the scaled Born cross sections for individual vibrational excitations of carbon monoxide (CO) in the article following the present one[15] (referred to as Paper III). Note that the scaling of Born cross sections is valid only for integral cross sections of electric dipole-allowed excitations.

Unlike the case we have just described for electron scattering from H_2O, there have been significant theoretical and experimental studies looking at the spectroscopy of the electronic states in water.[16–34] These studies are not simply noted here for completeness, as we shall shortly see they were vital in enabling us to deconvolve the respective electronic-state contributions to the measured energy-loss spectra. A summary of the major results from Refs. 16–34 can be found in Table X of Itikawa and Mason.[6] In both the molecular spectroscopy case and for the scattering calculations, an important first test to verify the quality of target wave functions is to compare the length and velocity forms of calculated oscillator strengths to corresponding accurate experimental values. For the optical oscillator strength (OOS) for excitation of the $\tilde{A}\,^1B_1$ electronic state from the $\tilde{X}\,^1A_1$ ground state, there are theoretical[20,35–39] and experimental[32,40–44] data available in the literature. In general we find differences in the OOS values within the theories and within the experiments and between the existing theories and experiments. Therefore, we have also attempted to try and clarify this situation by experimentally determining an accurate value for the OOS of the $\tilde{A}\,^1B_1$ state as a part of this work.

Experimental details are described in Sec. II, scaling of the Born cross section is summarized in Sec. III, results and discussions are presented in Sec. IV, and conclusions are stated in Sec. V.

II. EXPERIMENTAL DETAILS

In this paper we report results from independent measurements made at Sophia University and Flinders University. We therefore sequentially discuss the respective apparatus used to take the data that we will shortly describe.

A. Flinders University

A high-resolution electron monochromator, described originally by Brunger and Teubner,[45] was employed to make the measurements. Here a beam of H_2O, effusing from a molybdenum tube of 0.6 mm internal diameter, is crossed with a beam of pseudomonoenergetic electrons of desired energy T. Elastically and inelastically scattered electrons at a particular scattering angle (θ) are energy analyzed and detected. The overall energy resolution of the monochromator for these experiments was ~50 meV [full width at half maximum (FWHM)] and, under normal operating conditions, incident electron-beam currents of ~2 nA were obtained in the interaction region for the energy range of the Flinders measurements. As in previous work[45] the true zero scattering angle was determined as that about which the elastic scattering intensity was symmetric. The estimated error in this determination is ±1°. The electron energy scale was calibrated against the well-known helium $2\,^2S$ resonance at 19.367 eV and is estimated to be accurate to better than 50 meV.

At each incident energy in the range of 20–50 eV, energy-loss spectra were recorded at each scattering angle over the range of −0.5–12 eV. A typical spectrum (with the elastic peak suppressed for clarity) is shown in Fig. 1(a). The spectra were obtained by ramping the analyzer in an energy-loss mode in conjunction with a multichannel scalar which stored the scattered signal as a function of energy loss. The data were then transferred to a 433 MHz workstation for analysis. Each spectrum was then analyzed (deconvolved) by a computer least-squares fitting technique that is similar in detail to that outlined by Nickel *et al.*,[46] although adapted to accommodate the particular spectroscopy of H_2O.[16–34] In particular, the peak positions, profile shapes, and widths used in our deconvolution were gleaned and fixed as much as possible from the earlier work.[16–34] An example of our spectral deconvolution is also given in Fig. 1(a). In practice the fitting procedure yielded the ratio of the DCS for the inelastic feature of interest ($\tilde{A}\,^1B_1$ in this case, n' in general), $\sigma_{n'}(T,\theta)$, to the elastic differential cross section $\sigma_0(T,\theta)$. That is,

$$R_{n'}(T,\theta) = \frac{\sigma_{n'}(T,\theta)}{\sigma_0(T,\theta)}. \tag{1}$$

It is immediately apparent from Eq. (1) that the product $R_{n'}(T,\theta) \times \sigma_0(T,\theta)$ then gives the required electronic state differential cross section provided $\sigma_0(T,\theta)$ is known. In the present study our preferred elastic H_2O differential cross sections are the recent results from Cho *et al.*[47] Equation (1) is only valid if the transmission efficiency of the analyzer remains constant over the energy loss and angular range studied, or is at least well characterized. Unlike our previous study on CO_2,[48] in this work we determine the behavior of the analyzer response function following the philosophy outlined recently by Allan.[49]

Particular attention to the identification and quantification of all possible sources of error has been made throughout these measurements, with a general discussion of these sources of error being found in Brunger and Buckman.[50] In

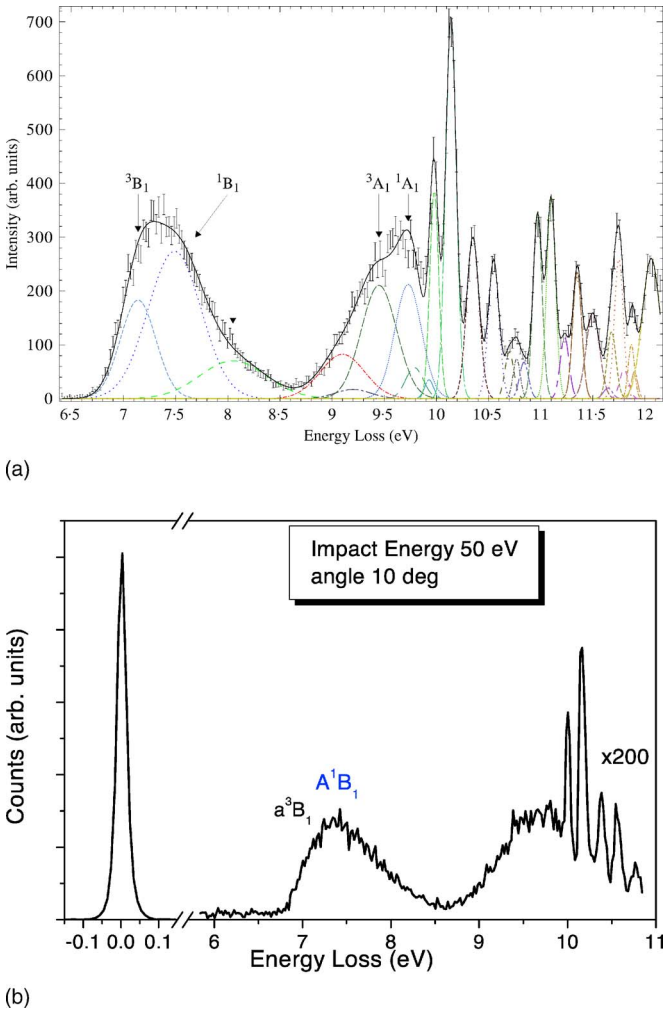

FIG. 1. (Color online) (a) Typical energy-loss spectrum for electron-impact excitation of the electronic states of water. $T=30$ eV and $\theta=10°$. Note that the elastic peak has been suppressed for the sake of clarity. Also shown in this figure is our spectral deconvolution of this energy-loss spectrum (see text for details). (b) Typical energy-loss spectrum as measured at Sophia University. $T=50$ eV and $\theta=10°$.

this case the statistical errors associated with the scattering intensity measurements are small (<2%). Additional errors due to the uncertainty in the elastic cross section by Cho *et al.*[47] (~10%) and our analyzer transmission calibration (~15%) must also be considered. Another important error in our study is that associated with the numerical deconvolution of the energy-loss spectra, with the overall errors on our DCS typically ranging from 18% to 30%, depending on the T and θ under consideration.

B. Sophia University

The experimental apparatus and procedures used at Sophia University have also been described in detail previously,[51] so we will not repeat them again here. Briefly, however, the spectrometer consists of an electron gun with a hemispherical monochromator, a molecular beam, and a rotatable detector ($\theta=-10°-130°$) with a second hemispherical system. All these components are employed in a crossed-beam configuration with the electron-beam crossing the effusive molecular beam at right angles. A number of tube lenses in the spectrometer have been used for imaging and energy control of the electron beam, whose characteristics were carefully modeled by electron trajectory calculations. Both the monochromator and analyzer are enclosed in differentially pumped boxes to reduce the effect of background gases and to minimize any stray electron background. The target molecular beam is produced by effusing H_2O through a simple nozzle with an internal diameter of 0.3 mm and length of 5 mm. Note that the spectrometer and nozzle are heated to a temperature of ~70 °C to avoid any "sticking" of the gas sample.

The energy resolution of the Sophia spectrometer was typically 30–35 meV (FWHM) and the angular resolution was about ±1.5° (FWHM). The primary electron-beam current was in the range of 3–9 nA, depending on the actual beam energy which was in the range $T=20-200$ eV. We note that voltages for both the input and output lenses of the hemispheres were carefully adjusted to ensure the base resolution of the energy-loss spectra remained as symmetric as possible. We further note that the energy calibration (±35 meV) and zero scattering angle calibration (±1°) were, respectively, performed in the same manner as at Flinders. A typical example of an energy-loss spectrum measured at Sophia University is given in Fig. 1(b). Note that the elastic peak has been included in this case.

Two normalization procedures were adopted to place the energy-loss spectra taken at Sophia on an absolute scale. The first is essentially identical to that previously described for Flinders, while in the second intensity ratios for the electronic excitation in H_2O relative to that for the excitation of the $2\,^1P$ state in He were used. The "standard" $2\,^1P$ differential cross sections were then employed to fix the corresponding absolute scale of the H_2O electronic states.[52] Great care was also taken at Sophia University to establish the transmission of the analyzers over the relevant energy-loss range, with full details of this procedure being found in Kitajima *et al.*[51] At 20–50 eV there is a potential $^3B_1$ contribution to the $^1B_1$ signal (see Fig. 1), so that these data were sent to Flinders for deconvolution. At 100 and 200 eV and the very forward scattering angles of measurement ($\theta=3.5°-11°$), the $^3B_1$ contamination was negligible so that this precaution was unnecessary.

All the energy-loss spectra were carefully measured in order to obtain sufficient intensity for the electronic excitation spectra. Experimental errors, including a figure of ~10% for the elastic DCSs,[47] are estimated to be of the order of ±31% for the electronic-state excitation cross sections. Note that where applicable this latter estimate includes an error for the deconvolution of the energy-loss spectra.

III. SCALED BORN CROSS SECTIONS

Scaled (plane-wave) Born cross sections for integral cross sections of dipole-allowed excitations—*f* scaling and *BE* scaling—are described in detail in Paper I. Born cross sections are not only subject to the approximation in the collision theory part but also depend on the accuracy of the wave functions used for the initial and final states of the target molecule.

The f-scaled Born cross section σ_f is given by

$$\sigma_f(T) = \frac{f_{\text{accur}}}{f_{\text{Born}}}\sigma_{\text{Born}}(T), \tag{2}$$

where T is the incident electron energy, f_{accur} is an accurate dipole f value from accurate wave functions or experiments, and f_{Born} is the dipole f value from the same wave functions used to calculate the unscaled Born cross section σ_{Born}. The f scaling has the effect of replacing the wave functions used for σ_{Born} with accurate wave functions, i.e., σ_f is equivalent to the Born cross section calculated with accurate wave functions.

The BE-scaled Born cross section σ_{BE} is given by

$$\sigma_{BE}(T) = \frac{T}{T+B+E}\sigma_{\text{Born}}(T), \tag{3}$$

where B is the binding energy of the electron being excited, and E is the excitation energy.

The BE scaling corrects the deficiency of the Born approximation, i.e., converts σ_{Born} into cross sections reliable at low T without losing the well-known validity of the Born approximation at high T.

If an unscaled σ_{Born} is obtained from poor wave functions while an accurate f value is known, then both f scaling and BE scaling can be applied to obtain a BEf-scaled Born cross section σ_{BEf},

$$\sigma_{BEf}(T) = \frac{f_{\text{accur}}T}{f_{\text{Born}}(T+B+E)}\sigma_{\text{Born}}(T). \tag{4}$$

Articles that report unscaled Born cross sections for molecules usually present the theoretical data in the form of dimensionless generalized oscillator strengths (GOSs), $G(Q)$, tabulated as functions of momentum transfer squared Q defined by

$$Q = (k_i a_0)^2 + (k_f a_0)^2 - 2(k_i a_0)(k_f a_0)\cos\theta, \tag{5}$$

where k_i and k_f are the initial and final momenta of the incident electron, a_0 is the Bohr radius (0.529 Å), and θ is the scattering angle of the incident electron.

The GOS is used to derive differential cross sections. Since the scaling methods described above are valid only for integral cross sections, it is convenient to have a GOS in an analytic form so that the GOS can be integrated over the momentum transfer to produce integral cross sections for arbitrary incident energy T.

As is discussed in Paper I, Vriens[53] proposed the following formula to represent a GOS for a dipole-allowed excitation based on the analytic properties identified by Lassettre[54] and Rau and Fano:[55]

$$G(x) = \frac{1}{(1+x)^6}\left[\sum_{m=0}^{\infty}\frac{f_m x^m}{(1+x)^m}\right], \tag{6}$$

where

$$x = Q/\alpha^2, \tag{7}$$

and

$$\alpha = \sqrt{B/R} + \sqrt{(B-E)/R}. \tag{8}$$

In Eq. (6), f_m are fitting constants, and in Eq. (8) R is the Rydberg energy (13.6 eV). At the $x=0$ optical limit, the value of $G(0)=f_0$ should be set to the OOS, f. Although Lassettre[54] identified α as shown in Eq. (8) from the analytic properties of the GOS, the binding energy B of an electron in a many-electron molecule can be defined only in the context of a simple independent particle model. For a GOS calculated from multiconfiguration wave functions, it is better to simply take α^2 as a fitting constant along with f_m. To fit a theoretical GOS, the OOS $f=f_0$ in Eq. (6) should be the one obtained with the same wave functions as those used to calculate the GOS.

A GOS for a dipole-allowed excitation usually peaks at the optical limit, i.e., $Q=0$. Sometimes a GOS has a second peak at a large Q value, when the wave functions have radial nodes. When the GOS with such an extra peak is tabulated with enough data points, Eq. (6) with several terms can reproduce the GOS well including the secondary peak.

The same analytic formula can be used to fit and extrapolate experimental DCS to the forward and backward angles not observed in the experiment, and then to integrate the DCS. As is shown later, even f_0 should be treated as a fitting constant when fitting to experimental DCSs.

"Experimental" GOS can be obtained by substituting experimental DCS, $\sigma(T,\theta)$, into the relation between theoretical DCS and GOS:

$$G_{\text{exp}}(Q) = \frac{(E/R)k_i a_0}{4a_0^2 k_f a_0}Q\sigma(T,\theta), \tag{9}$$

At low T, experimental GOSs often have secondary peaks as will be shown later. These secondary peaks have a totally different origin than those seen in the theoretical GOS; the former come from interactions not represented in the Born approximation—such as the interference between the direct and exchange amplitudes—while the latter come from the radial nodes in wave functions. Hence, secondary peaks in experimental GOS at low T cannot be fitted well by the extra terms in Eq. (6). Instead, the following function with two fitting constants b and c in addition to the leading fraction in Eq. (6) was found to represent the experimental GOS at low T well:

$$g(x) = bx\exp(-cx). \tag{10}$$

Integral cross sections are now obtained by integrating the GOS over the limits of Q corresponding to $\theta=0°$ and 180°:

$$\sigma_{\text{Born}}(T) = \frac{4\pi a_0^2}{T/R}\int_{Q_{\text{min}}}^{Q_{\text{max}}}\frac{G(Q)}{E/R}d(\ln Q), \tag{11}$$

with

$$Q_{\text{min}} = 2\frac{T}{R}\left[1 - \frac{E}{2T} - \sqrt{1-\frac{E}{T}}\right],$$
$$Q_{\text{max}} = 2\frac{T}{R}\left[1 - \frac{E}{2T} + \sqrt{1-\frac{E}{T}}\right]. \tag{12}$$

TABLE I. Constants to be used with Eq. (6) to reproduce the theoretical (Ref. 57) and experimental generalized oscillator strengths (GOSs). The original f value calculated from wave functions is $f=0.046$, and the α^2 value for the experimental GOS is from Eq. (7). The binding energy B and excitation energy E are from Berkowitz (Ref. 58). T is the incident electron energy, and the rest of the constants were obtained by least-squares fitting.

B (eV)	E (eV)		
12.62	7.4		
		Experimental GOS	
Constant	Theoretical GOS	$T=100$ eV	$T=200$ eV
f_0	0.046 29	0.0458	0.045 97
α^2	5	2.5035	2.503 5
f_1	−0.455 06	−5.9901±0.8985	−10.7339±2.0253
f_2	1.077 7	276.63±96.87	863.57±355.83
f_3	1.497 2		
f_4	−7.961 7		
f_5	10.189		

Two different sets of theoretical GOS for the $\tilde{A}\ ^1B_1$ excitation are available in the literature. Bhanuprakash *et al.*[56] calculated GOS with multiconfiguration wave functions, and Durante *et al.*[57] used wave functions from the random phase approximation. The f value from the GOS by Bhanuprakash *et al.* is 0.054, while the f value from the GOS by Durante *et al.* is 0.046, which is in excellent agreement with the f value recommended by Berkowitz[58] based on his f sum-rule analysis. Hence, we chose the theoretical GOS by Durante *et al.* to generate unscaled Born cross sections and apply the *BE* scaling to obtain integral cross sections valid at low and high T. The fitting of the GOS calculated by Durante *et al.*[57] required a total of six terms ($m=5$) in Eq. (6). In Table I, we present the values of f and f_m used with Eq. (6) to fit the original GOS calculated by Durante *et al.*,[57] and the fitted GOS is compared to the original GOS by Durante *et al.* in Fig. 2.

IV. RESULTS AND DISCUSSION

A. Differential cross sections

In Figs. 3–6 and Table II we present our DCSs for the excitation of the $\tilde{A}\ ^1B_1$ electronic state in H_2O. There are several general trends that we can elucidate from Figs. 3–6. These include that all the DCSs are strongly forward peaked as is expected from an electric dipole-allowed—though dissociative—excitation, and also perhaps a result of both the strong permanent dipole moment (1.854 D=6.18 $\times 10^{-30}$ C m) and significant dipole polarizability ($9.79a_0^3$) of water, with the degree of forward peaking increasing as the beam energy is increased. Finally, to within their respective stated uncertainties, it is apparent that the independent Sophia and Flinders data are largely consistent with one another. When one also allows for the ±1° uncertainty in the

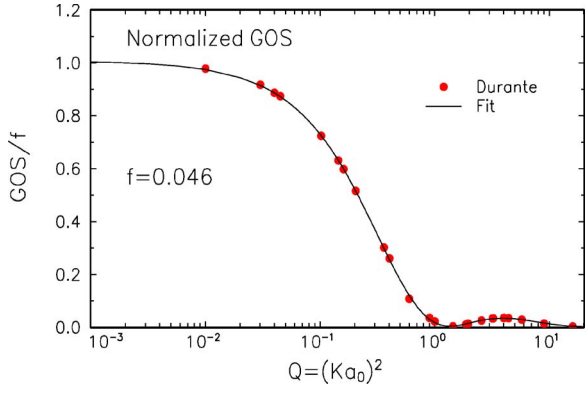

FIG. 2. (Color online) Comparison of the original generalized oscillator strength (GOS) by Durante *et al.* (Ref. 57) and the fitted GOS using Eq. (6) The ordinate is the normalized theoretical GOS, i.e., GOS divided by the optical $f=0.046$ (see Table I for the fitting constants).

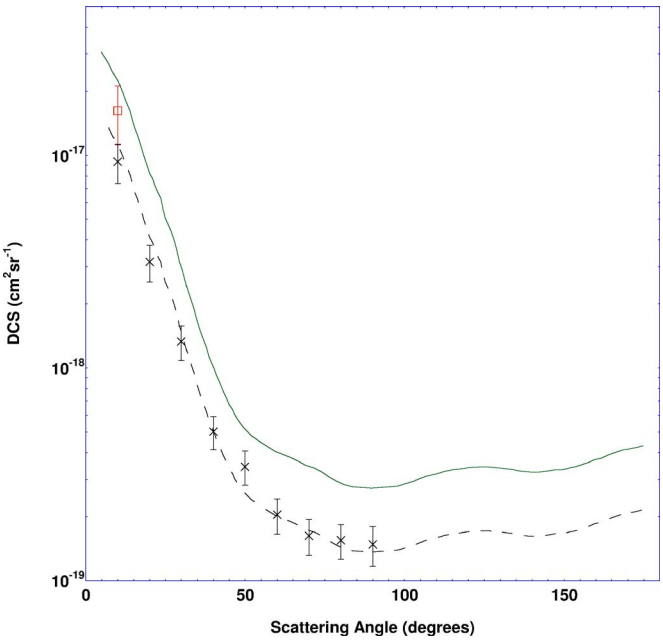

FIG. 3. (Color online) Present differential cross sections (cm^2/sr) for excitation of the $A\ ^1B_1$ electronic state in water at $T=20$ eV. Crosses, Flinders DCS; squares, Sophia DCS; solid curve, complex Kohn cross section by Gil *et al.* (Ref. 9) at $T=20$ eV; and dashed curve, the cross section by Gil *et al.* multiplied by 0.5.

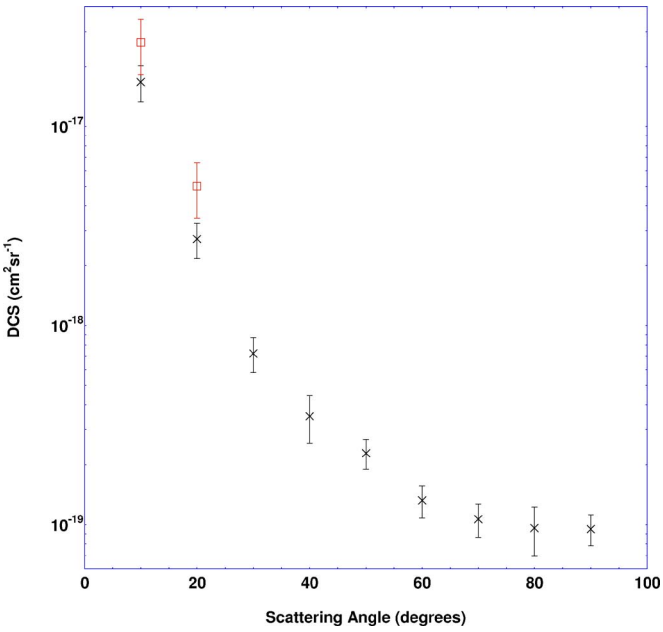

FIG. 4. (Color online) Same as Fig. 3, but at $T=30$ eV.

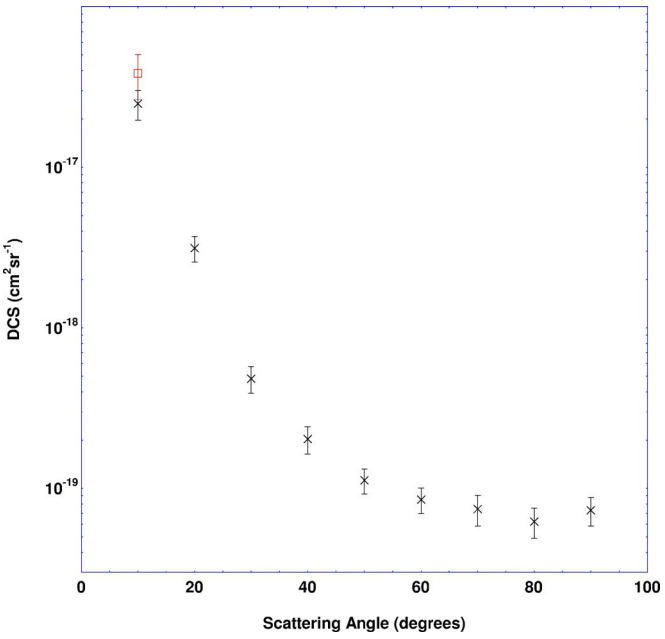

FIG. 5. (Color online) Same as Fig. 3, but at $T=40$ eV.

zero angle calibration of each spectrometer, which is potentially critical with the sharp slope of the DCS at the forward angles, then the agreement between Flinders and Sophia is actually very good. Note, however, that the data in Figs. 3–6 do suggest that the Sophia DCS might be somewhat systematically larger in magnitude than that of Flinders at the angles where the cross-check measurements were made. This does have some implications to the ICSs we derive later (see Sec. IV C).

In Fig. 3, at $T=20$ eV, we can also compare the present DCS with a complex Kohn calculation from Gil *et al.*[9] Here we find that the calculation systematically overestimates the magnitude of the measured DCS (by a factor of ~2) across the common angular range. On the other hand the shapes of the measured and calculated angular distributions are in very good accord. To illustrate this latter point we have scaled the theory in Fig. 3 by a factor of ~0.5. One possible explanation for the discrepancy between the calculation and our measurements at 20 eV has been advanced by Rescigno.[59] He noted that the $\tilde{A}\ ^1B_1$ state is an example of a "Valberg" state, namely, it has both Rydberg and valence characters that would be very difficult to characterize properly with the relatively simple description of the target used by Gil *et al.*[9] Another possibility might be that a fixed nuclei (FN) description for the scattering framework is inadequate, rather an adiabatic nuclei (AN) approach might be required. There is some anecdotal evidence in support of this latter proposition. A long-standing discrepancy, for the excitation of the $b^3\Sigma_u^+$ electronic state in H_2, between the ICS measurements of Khakoo and Segura[60] and various FN-level calculations[61] was only resolved when Trevisan and Tennyson[61] applied an AN-*R*-matrix approach to the problem. However, when Gorfinkiel *et al.*[8] extended the earlier FN-*R*-matrix H_2O results of Morgan[7] to the AN level, they observed little effect on the ICS of the $\tilde{A}\ ^1B_1$ state. Notwithstanding this, Rescigno[59] further noted that while Gorfinkiel *et al.*[8] tried to employ more sophisticated target wave functions and an AN-*R*-matrix approach, they possibly failed to appreciate that the mixed Rydberg-valence character of the states involved would require a bigger *R*-matrix box than they typically use. As a consequence, the calculation of Gorfinkiel *et al.*[8] might not be definitive in ruling out a FN versus AN rationale for the discrepancy observed in Fig. 3.

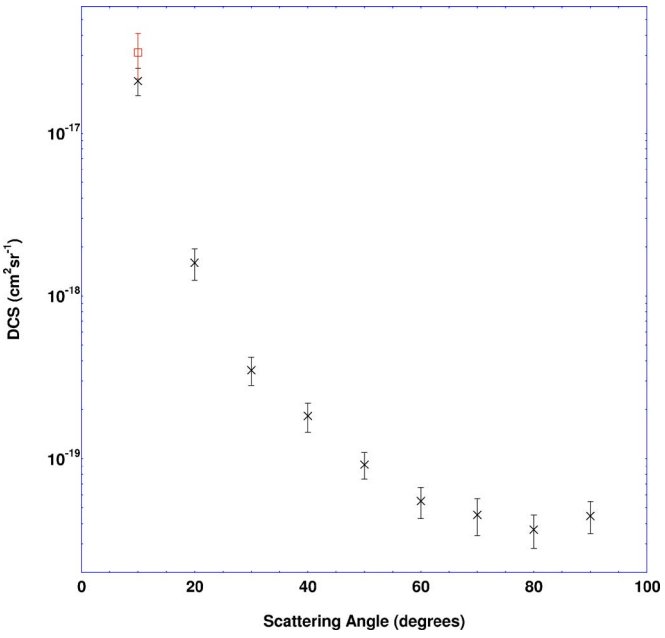

FIG. 6. (Color online) Same as Fig. 3, but at $T=50$ eV.

B. Experimental generalized oscillator strengths and the optical oscillator strength

At $T=100$ and 200 eV, using the $\sigma(T,\theta)$ derived from their energy-loss spectra, experimental GOS, $G_{\text{expt}}(Q)$, has been determined for the $\tilde{A}\ ^1B_1$ excitation at Sophia University with Eq. (9). The experimental GOS values are listed in Table III and plotted in Fig. 7.

Based on the information in Table III, an optical oscillator strength was also determined for the $\tilde{A}\ ^1B_1$ excitation. This was achieved by fitting the experimental GOS with Eq. (6) using three terms in the expansion. The fitting constants are tabulated in Table I, and our fit to the 100 and 200 eV GOS data is plotted as a solid line in Fig. 7.

The experimental OOS for the $\tilde{A}\ ^1B_1$ excitation, as derived using the above procedure, is given in Table IV along with a comparison of some of the results from previous experiments[32,40–44,58] and calculations.[20,35–39] The present OOS value of $f=0.0459\pm0.0069$ is in excellent agreement with the photoabsorption results from Lee and Suto[42] and Yoshino *et al.*,[43,44] and the f sum-rule adjusted value recommended by Berkowitz,[58] and in good accord with the high-resolution dipole (e,e) value from Chan *et al.*[32] We therefore believe that the OOS for the $\tilde{A}\ ^1B_1$ excitation of H_2O is well established. This is important as the OOS represents a good test[62] for any structure calculation seeking to accurately represent the wave functions for this excitation. In this respect

TABLE II. Differential cross sections (DCSs) for electron-impact excitation of the $\tilde{A}\ ^1B_1$ electronic state of water as functions of the incident electron energy T. The column heading F refers to Flinders data and S to Sophia data. The percentage uncertainties of the DCS are given in parentheses.

	$\sigma(\theta)$ (10^{-19} cm^2/sr)							
	T=20 eV		T=30 eV		T=40 eV		50 eV	
θ (deg)	F	S	F	S	F	S	F	S
10	93.4 (22.7%)	162 (31%)	167.3 (22.4%)	264 (31%)	248.6 (23%)	384 (31%)	210.1 (20.4%)	288 (31%)
20	31.6 (21.1%)		27.2 (21.8%)	50.2 (31%)	31.4 (19.2%)		16.0 (28.5%)	
30	13.3 (19.8%)		7.25 (21.3%)		4.82 (29.5%)		3.5 (21.4%)	
40	5.02 (18.8%)		3.51 (27.8%)		2.03 (20.7%)		1.83 (22%)	
50	3.44 (19.4%)		2.29 (17.8%)		1.12 (18.8%)		0.92 (20%)	
60	2.04 (20.1%)		1.32 (19.5%)		0.85 (19.3%)		0.55 (23.6%)	
70	1.63 (20.5%)		1.06 (20.6%)		0.75 (23.5%)		0.45 (27.8%)	
80	1.55 (19.7%)		0.96 (30.2%)		0.62 (23.2%)		0.37 (25.2%)	
90	1.48 (23%)		0.95 (18.8%)		0.73 (21.8%)		0.45 (24.3%)	

we note the very good agreement (see Table IV) between the present OOS and the calculated length and velocity results from Phillips and Buenker.[39]

We were able to fit the GOS data at T=100 and 200 eV using the formula of Vriens,[53] which was designed to represent the theoretical Born cross sections, and also obtained the correct OOS at the Q=0 limit. However, the comparison of experimental and theoretical ICSs indicates that the Born approximation is still ~10% higher than experiment at T =200 eV, as is discussed in Sec. IV C.

C. Integral cross sections from the present differential cross sections

The present integral cross sections for excitation of the $\tilde{A}\ ^1B_1$ state are listed in Table V and plotted in Fig. 8. Also included in Fig. 8 are the corresponding calculations from Gil *et al.*,[9] and Gorfinkiel *et al.*,[8] and the Born and *BE*-scaled Born cross sections[14] that were determined as a part of the present study (see Sec. III for details).

In Table V two sets of "present ICS" are given. The first set is from the application of the molecular phase shift analysis (MPSA) procedure of Campbell *et al.*[63] to the Flinders DCS, while the second set is an application of Eqs. (6)–(10) to "optimum" DCS constructed by combining the Flinders and Sophia data at T=20–50 eV, and from the Sophia data at 100 and 200 eV. Both these procedures extrapolate the measured DCS to 0°–180°, prior to integration, to obtain the required ICS. The experimental DCSs were fitted to analytic forms using only the first term in Eqs. (6) and (10) while the values of f_0=f, α^2, b, and c were determined by least-squares fitting. The values of these fitted constants used to obtain integral cross sections are listed in Table VI.

Note that all the $\tilde{A}\ ^1B_1$ DCSs are very strongly forward peaked, so that the major contributions to the integrand come from those angular regions where the DCS measurements are available. The present optimum DCSs, at each energy in the range of 20–50 eV, were simply constructed by renormalizing the Flinders data using the ratio between the Sophia DCS at 10° to the Flinders DCS at 10°. In this sense the ICS

TABLE III. Present generalized oscillator strength (GOS) vs momentum transfer square Q defined by Eq. (5). The percentage uncertainties of the GOS are given in parentheses.

	GOS	
Q	T=100 eV	T=200 eV
0.032 52	0.040 52 (15%)	
0.047 64		0.038 18 (15%)
0.052 16	0.031 93 (15%)	
0.073 26	0.029 48 (15%)	
0.078 63		0.031 76 (15%)
0.098 65	0.028 98 (15%)	
0.121 19		0.026 11 (15%)
0.157 5		0.024 52 (15%)
0.209 95		0.017 31 (15%)
0.251 94	0.017 47 (15%)	
0.276 98		0.014 05 (15%)

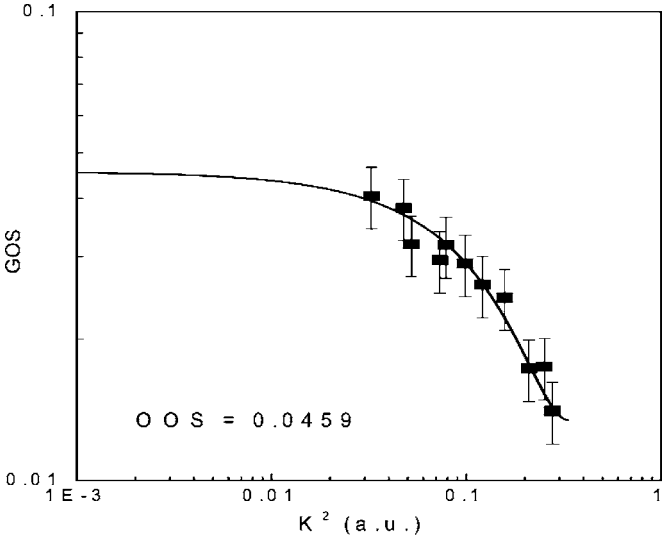

FIG. 7. (Color online) Experimental generalized oscillator strengths as functions of the momentum transfer squared, Q=$(Ka_0)^2$. Squares, Sophia data. The fit to these data using Eq. (6) is also shown (see Table I for the fitting constants).

TABLE IV. Comparison between the present experimental optical limit f of the GOS for the excitation of the $\tilde{A}\,^1B_1$ electronic state of water, with a selection of those from other measurements and calculations. Note that the theoretical dipole length f_l and dipole velocity f_v results are both shown.

	OOS		
Source	f_l	f	f_v
Philips and Buenker (Ref. 39)	0.050 0		0.0576
Bhanuprakash *et al.* (Ref. 56)		0.054	
Durante *et al.* (Ref. 57)		0.046	
Theodorakopoulous *et al.* (Ref. 38)		0.065	
Diercksen *et al.* (Ref. 20)	0.020 79		
Williams and Langhoff (Ref. 37)	0.036		
Buenker and Peyerimhoff (Ref. 36)	0.059 2		0.0779
Wood (Ref. 35)	0.037		
Yoshino *et al.* (Refs. 43 and 44)		0.0460	
Chan *et al.* (Ref. 32)		0.0497	
Lee and Suto (Ref. 42)		0.0456	
Lassettre and White (Ref. 41)		0.060	
Laufer and McNesby (Ref. 40)		0.041	
Berkowitz (Ref. 58)		0.0460	
Present result		0.0459±0.0069	

derived using Eqs. (6)–(10) represents an upper bound on the $\tilde{A}\,^1B_1$ ICS for the DCS data given in Table II. Similarly, the MPSA set of ICS represents a lower bound on the $\tilde{A}\,^1B_1$ ICS. Not surprisingly, there are important differences between the two sets of present ICS, which simply reflects the range in possible values for this excitation process given the measured DCS in Table II. In any event, however, we note that the two sets of present ICS almost overlap with each other, at each energy, to within their stated error limits (±25% for the Flinders data and ±31% for the Sophia data).

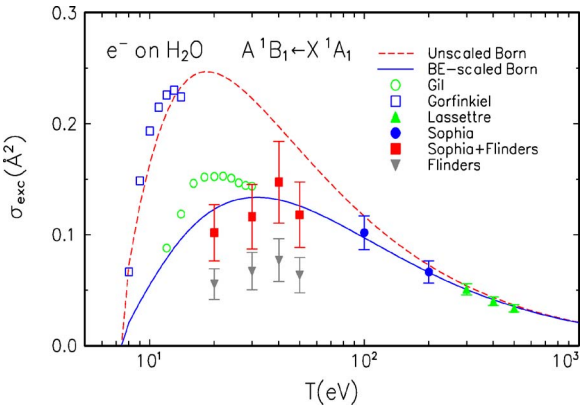

FIG. 8. (Color online) Comparison of experimental and theoretical integral cross sections for the excitation of the $\tilde{A}\,^1B_1$ electronic state in water. Dashed curve, unscaled Born cross section; solid curve, *BE*-scaled Born cross sections; open circles, complex Kohn cross section by Gil *et al.* (Ref. 9); open squares, AN-*R* matrix cross section by Gorfinkiel *et al.* (Ref. 8); upright triangles, experimental data by Lassettre and co-workers (Refs. 64 and 65); filled circle, experimental data from Sophia; filled squares, combined data from Sophia and Flinders; and inverted triangles, data from Flinders.

D. Integral cross sections from the differential cross sections by Lassettre

More than 30 years ago, Lassettre and co-workers measured the DCS of the $\tilde{A}\,^1B_1$ excitation of H_2O,[41,64,65] but they published their data in the form of experimental GOS using Eq. (9). Their goal was to determine the optical limit, and they obtained an average value of $f=0.060$ from DCSs measured at $T=300-600$ eV. Among these, we used the experimental GOS by Lassettre and Skerbele[64] at $T=300$ and 400 eV, and the experimental GOS by Klump and Lassettre[65] at $T=500$ eV. The GOS by Klump and Lassettre

TABLE V. Integral cross section (ICSs) for electron-impact excitation of the $\tilde{A}\,^1B_1$ electronic state of water as a function of the incident electron energy T. The column marked MPSA refers to data determined at Flinders using their molecular phase shift analysis procedure, $S+F$ refers to the ICS derived from the combined data from Sophia and Flinders using the normalization of the Sophia data σ_{BE} refers to the *BE*-scaled Born cross section (see Sec. III), σ_{Born} refers to the unscaled Born cross section from the generalized oscillator strength reported by Bhanupraksh *et al.* (Ref. 56), Sophia refers to the ICS derived from the Sophia data, and Lassettre refers to the f-scaled integral cross sections obtained from experimental GOS by Lassettre and co-workers (Refs. 64 and 65). The percentage uncertainties of the ICSs are given in parentheses.

	ICS (10^{-17} cm^2)					ICS (10^{-17} cm^2)			
T	MPSA	S+F	σ_{BE}	σ_{Born}	T (eV)	Sophia	Lassettre	σ_{BE}	σ_{Born}
10			0.5457	1.6380	100	1.017 (18%)		0.9718	1.1663
15			1.0260	2.3653	200	0.663 (18%)		0.6590	0.7249
20	0.554 (25%)	1.018 (31%)	1.2293	2.4596	300		0.0507 (10%)	0.5048	0.5385
25			1.3108	2.3603	400		0.0399 (10%)	0.4126	0.4332
30	0.671 (25%)	1.162 (31%)	1.3357	2.2270	500		0.0334 (10%)	0.3507	0.3648
35			1.3324	2.0945	600			0.3062	0.3164
40	0.770 (25%)	1.473 (31%)	1.3143	1.9721	700			0.2724	0.2802
45			1.2885	1.8617	800			0.2458	0.2520
50	0.635 (25%)	1.178 (31%)	1.2588	1.7627	900			0.2243	0.2293
55			1.2273	1.6740	1000			0.2065	0.2107
60			1.1954	1.5943	2000			0.1183	0.1195
70			1.1331	1.4571	3000			0.0846	0.0851
80			1.0746	1.3435	4000			0.0665	0.0668
90			1.0209	1.2479	5000			0.0550	0.0553

TABLE VI. Constants used to fit experimental generalized oscillator strengths (GOSs) from the present work and from Lassettre and co-workers (Refs. 64 and 65) [see Eqs. (6), (7), and (10)].

		Fitting constants		
T (eV)	Dipole $f=f_0$	α^2	b	c
20	0.0132	1.7	0.0029	0.1
30	0.021	1.47	0.0025	0.21
40	0.036	1.31	0.0012	0.13
50	0.035	1.15	0.0006	0.1
100	0.046	1.2		
200	0.046	1.3		
300	0.060	1.4		
400	0.060	1.27		
500	0.0675	1.21	0.0009	0.11

covered large enough values of Q to reveal the secondary maximum in the GOS similar to the one in Fig. 2.

As we have done with the present DCSs, we used our own fitting to the GOS by Lassettre and co-workers, i.e., using only the first term of Eq. (6) for $T=300-500$ eV and Eq. (10) only for $T=500$ eV while treating f, α^2, b, and c as fitting constants. These fitting constants are also listed in Table VI. Since the "correct" value of the OOS is $f=0.0460$, we applied the f scaling to the ICSs obtained from the experimental GOS by Lassettre and co-workers. These f-scaled ICSs from the experimental GOS by Lassettre and co-workers are included in Table V and Fig. 8.

E. Discussion on integral cross sections

It is clear from Fig. 8 that, over the range of energy overlap, neither of the R-matrix calculations,[7,8] nor the complex Kohn calculation[9] (except at 30 eV), nor the present unscaled Born cross section does a particularly good job of reproducing the experimental ICS. In the case of the R-matrix and complex Kohn calculations, possible reasons for this discrepancy are well canvassed by Gorfinkiel *et al.*[8] These include inherent limitations in the AN and FN approaches, the use of a one-dimensional model to treat the nuclear motion, and a limitation in the diffuseness of the wave functions describing the target states. As a consequence Gorfinkiel *et al.* noted that the polarizability of the molecule may not be accurately reproduced so that the quality of the representation of these states with Rydberg character would be undermined. Only the present *BE*-scaled cross section provides a reasonable description of the $\tilde{A}\ ^1B_1$ ICS for the energy range of interest, a quite remarkable result given the complexity of the scattering system and the relative simplicity of this model.[14] Indeed the present experimental ICSs, determined from the optimum DCS and Eqs. (6)–(9) and those derived from the earlier data of Lassettre and White,[41] agree with the *BE*-scaled result to typically better than 25% from $T=20$ to 500 eV.

Finally, we note that the results from an experiment by Harb *et al.*[66] in principle include contributions from the $^3B_1$, $^3A_1$, and $^1A_1$ states as well as the $\tilde{A}\ ^1B_1$ state. Hence, they represent an upper bound to the present measurements. Nonetheless we do not believe that the extent of the discrepancy in magnitude (about a factor of 20) between the present $\tilde{A}\ ^1B_1$ ICS and that of the data of Harb *et al.* can simply be explained by the contributions of the other states. The data of Harb *et al.* were placed on an absolute scale using the old dissociative attachment cross section values of Melton,[67] which according to Itikawa and Mason[6] may suffer from a systematic error. Hence it is possible that this might also explain, at least in part, the discrepancy between the two measurements.

V. CONCLUSIONS

We have reported on absolute differential and integral cross section measurements for electron-impact excitation of the $\tilde{A}\ ^1B_1$ electronic state of water. Independent measurements at Sophia and Flinders were found to be largely consistent with one another (to within their error limits), a point which gives us further confidence in the present data.

Agreement with existing theoretical calculations was typically found to be only marginal, the exception to this being the very good agreement found at the ICS level between the present data and the *BE*-scaled Born cross section calculated as a part of the current study. More theoretical input is still needed particularly for the differential cross sections. As is demonstrated in Paper III (Ref. 15) on the excitation cross sections of CO, the *BE*-scaled and *BEf*-scaled Born cross sections are in excellent agreement with the new measurements on CO at Sophia, old measurements at Flinders, and other experimental data available in the literature. Together with the evidence on H_2 presented in Paper I (Ref. 14) and those on CO in Paper III,[15] the experimental and theoretical ICSs in this article clearly establish the validity of the scaled Born cross sections.

We also derived the optical oscillator strength for the $\tilde{A}\ ^1B_1$ excitation from the $\tilde{X}\ ^1A_1$ ground state, which was in excellent agreement with that from a dipole (e,e) experiment,[32] photoabsorption experiments,[42–44] and the value recommended by Berkowitz.[58] Taken as a whole, we believe that the current theoretical and experimental studies represent a good first step to addressing the lack of available electronic-state excitation cross sections highlighted by Itikawa and Mason.[6]

ACKNOWLEDGMENTS

The work in Australia was supported by the Australian Research Council (ARC). The authors thank Marilyn Mitchell for typing this manuscript. One of the authors (M.A.B.) is grateful for the support of the Shahid Bahonar University of Kerman and Flinders University, which enabled him to participate in this work. The work at NIST was supported in part by the U.S. Department of Energy, Office of Fusion Sciences. They all thank Dr. Tom Rescigno for his useful comments on some aspects of this paper, and Professor Bill McConkey for providing tables of his data. They also acknowledge Dr. Casten Makochekanwa for his comments

on this work. His co-authors dedicate this paper to Dr. Yong-Ki Kim who was tragically killed in a car accident during the final stages of this work.

[1] X. Xie and M. J. Mumma, Astrophys. J. **386**, 720 (1992).
[2] M. A. Tas, E. M. van Veldhuizen, and W. R. Rutgers, J. Phys. D **30**, 1636 (1997).
[3] A. B. Meinel, Astrophys. J. **111**, 555 (1950).
[4] A. B. Meinel, Astrophys. J. **112**, 120 (1950).
[5] S. Uehara, H. Nikjou, and D. T. Goodhead, Radiat. Res. **152**, 202 (1999).
[6] Y. Itikawa and N. J. Mason, J. Phys. Chem. Ref. Data **34**, 1 (2005).
[7] L. A. Morgan, J. Phys. B **31**, 5003 (1998).
[8] J. D. Gorfinkiel, L. A. Morgan, and J. Tennyson, J. Phys. B **35**, 543 (2002).
[9] T. J. Gil, T. N. Rescigno, C. W. McCurdy, and B. H. Lengsfield III, Phys. Rev. A **49**, 2642 (1994).
[10] M.-T. Lee, S. E. Michelin, L. E. Machado, and L. M. Brescansin, J. Phys. B **26**, L203 (1993).
[11] M.-T. Lee, S. E. Michelin, T. Kroin, L. E. Machado, and L. M. Brescansin, J. Phys. B **28**, 1859 (1995).
[12] H. P. Pritchard, V. McKoy, and M. A. P. Lima, Phys. Rev. A **41**, 546 (1990).
[13] Y.-K. Kim, Phys. Rev. A **64**, 032713 (2001).
[14] Y.-K. Kim, J. Chem. Phys. **126**, 064305 (2007), preceding paper.
[15] H. Kato, M. Hoshino, H. Tanaka, M. J. Brunger, and Y.-K. Kim, J. Chem. Phys. **126**, 064307 (2007), following paper.
[16] C. R. Claydon, G. A. Segal, and H. S. Taylor, J. Chem. Phys. **54**, 3799 (1971).
[17] W. A. Goddard and W. J. Hunt, Chem. Phys. Lett. **24**, 464 (1974).
[18] N. W. Winter, W. A. Goddard, and F. W. Bobrowicz, J. Chem. Phys. **62**, 4325 (1975).
[19] P. Gurtler, V. Saile, and F. E. Koch, Chem. Phys. Lett. **51**, 386 (1977).
[20] G. H. F. Diercksen, W. P. Kraemer, T. N. Rescigno, C. F. Bender, B. V. McKoy, S. R. Langhoff, and P. W. Langhoff, J. Chem. Phys. **76**, 1043 (1982).
[21] U. Kaldor, J. Chem. Phys. **87**, 467 (1987).
[22] M. Warken, J. Chem. Phys. **103**, 5554 (1995).
[23] O. Christiansen, H. Koch, P. Jorgensen, and J. Olsen, Chem. Phys. Lett. **256**, 185 (1996).
[24] Z.-L. Cai, D. J. Tozer, and J. R. Reimers, J. Chem. Phys. **113**, 7084 (2000).
[25] R. van Harrevelt and M. C. van Hemert, J. Chem. Phys. **112**, 5777 (2000).
[26] H. Larsen, K. Hald, J. Olsen, and P. Jorgensen, J. Chem. Phys. **115**, 3015 (2001).
[27] A. B. Trofimov, G. Stelter, and J. Schirmer, J. Chem. Phys. **117**, 6402 (2002).
[28] A. Skerbele and E. N. Lassettre, J. Chem. Phys. **42**, 395 (1965).
[29] F. W. E. Knoop, H. H. Brogersma, and L. J. Oosterhoff, Chem. Phys. Lett. **13**, 20 (1972).
[30] S. Trajmar, W. Williams, and A. Kuppermann, J. Chem. Phys. **58**, 2521 (1973).
[31] A. Chutjian, R. I. Hall, and S. Trajmar, J. Chem. Phys. **63**, 892 (1975).
[32] W. F. Chan, G. Cooper, and C. E. Brion, Chem. Phys. **178**, 387 (1993).
[33] J. J. Jureta, Eur. Phys. J. D **32**, 319 (2005).
[34] R. Mota, R. Parafita, A. Giuliani *et al.*, Chem. Phys. Lett. **416**, 152 (2005).
[35] M. H. Wood, Chem. Phys. Lett. **28**, 477 (1974).
[36] R. J. Buenker and S. D. Peyerimhoff, Chem. Phys. Lett. **29**, 253 (1974).
[37] G. R. J. Williams and P. W. Langhoff, Chem. Phys. Lett. **60**, 201 (1979).
[38] G. Theodorakopoulous, I. D. Petsalakis, C. A. Nicolaides, and R. J. Buenker, J. Chem. Phys. **82**, 912 (1985).
[39] R. A. Phillips and R. J. Buenker, Chem. Phys. Lett. **137**, 157 (1987).
[40] A. H. Laufer and J. R. McNesby, Can. J. Chem. **43**, 3487 (1965).
[41] E. N. Lassettre and E. R. White, J. Chem. Phys. **60**, 2460 (1974).
[42] L. C. Lee and M. Suto, Chem. Phys. **110**, 161 (1986).
[43] K. Yoshino, J. R. Esmond, W. H. Parkinson, K. Ito, and T. Matsui, Chem. Phys. **211**, 387 (1996).
[44] K. Yoshino, J. R. Esmond, W. H. Parkinson, K. Ito, and T. Matsui, Chem. Phys. **215**, 429 (1997).
[45] M. J. Brunger and P. J. O. Teubner, Phys. Rev. A **41**, 1413 (1990).
[46] J. C. Nickel, P. W. Zetner, G. Shen, and S. Trajmar, J. Phys. E **22**, 730 (1989).
[47] H. Cho, Y. S. Park, H. Tanaka, and S. J. Buckman, J. Phys. B **37**, 625 (2004).
[48] M. A. Green, P. J. O. Teubner, L. Campbell *et al.*, J. Phys. B **35**, 567 (2002).
[49] M. Allan, J. Phys. B **38**, 3655 (2005).
[50] M. J. Brunger and S. J. Buckman, Nucleaus **34**, 201 (1997).
[51] M. Kitajima, S. Watanabe, H. Tanaka, M. Takekawa, M. Kimura, and Y. Itikawa, J. Phys. B **34**, 1929 (2001).
[52] S. Trajmar, J. M. Ratliff, G. Csanak, and D. C. Cartwright, Z. Phys. D: At., Mol. Clusters **22**, 457 (1992).
[53] L. Vriens, Phys. Rev. **160**, 100 (1967).
[54] E. N. Lassettre, J. Chem. Phys. **43**, 4479 (1965).
[55] A. R. P. Rau and U. Fano, Phys. Rev. **162**, 68 (1967).
[56] K. Bhanuprakash, P. Chandra, C. Chabalowski, and R. J. Buenker, Chem. Phys. **138**, 215 (1989).
[57] N. Durante, U. T. Lamanna, G. P. Arrighini, and C. Buidotti, Theor. Chim. Acta **90**, 115 (1995).
[58] J. Berkowitz, *Atomic and Molecular Photoabsorption: Absolute Total Cross Sections* (Academic, San Diego, 2002).
[59] T. N. Rescigno (private communication).
[60] M. A. Khakoo and J. Segura, J. Phys. B **27**, 2355 (1994).
[61] C. S. Trevisan and J. Tennyson, J. Phys. B **34**, 2935 (2001).
[62] B. H. Bransden and C. J. Joachain, *Physics of Atoms and Molecules* (Longman, London, 1983).
[63] L. Campbell, M. J. Brunger, A. M. Nolan, L. J. Kelly, A. B. Wedding, J. Harrison, P. J. O. Teubner, D. C. Cartwright, and B. McLaughlin, J. Phys. B **34**, 1185 (2001).
[64] E. N. Lassettre and A. Skerbele, J. Chem. Phys. **60**, 2464 (1974).
[65] K. N. Klump and E. N. Lassettre, Can. J. Phys. **53**, 1825 (1975).
[66] T. Harb, W. Kedzierski, and J. W. McConkey, J. Chem. Phys. **115**, 5507 (2001).
[67] C. E. Melton, J. Chem. Phys. **57**, 4218 (1972).